

## Effect of Nanorod Zinc Oxide on Electrical and Optical Properties of Starch-based Polymer Nanocomposites

M. Aizuddin Abdul Rahman<sup>1\*</sup>, Shahrom Mahmud<sup>1</sup>, Abdul Karim Alias<sup>2</sup>  
and Abdul Fauzi Mohd Nor<sup>3</sup>

<sup>1</sup>School of Physics, Universiti Sains Malaysia, 11800 USM Pulau Pinang, Malaysia

<sup>2</sup>School of Industrial Technology, Universiti Sains Malaysia,  
11800 USM Pulau Pinang, Malaysia

<sup>3</sup>School of Material and Mineral Resource Engineering, Engineering Campus,  
Universiti Sains Malaysia, 14300 Nibong Tebal, Seberang Perai Selatan,  
Pulau Pinang, Malaysia

\*Corresponding author: aizuddin.abdul.rahman@gmail.com

**Abstract:** *Sago starch (SS) based polymer nanocomposites (PNCs) were produced with presence of inorganic nanofiller (zinc oxide nanorods). The percentage of zinc oxide nanorods (ZnO-N) was varied from zero to 10 wt% with increment of 2%. Dielectric and conductivity behaviour of SS/ZnO-N polymer nanocomposites were characterised using LCR-frequency analyser. Structural and composition of ZnO-N filler and PNCs were characterised using field emission scanning electron microscope (FESEM), transmission electron microscope (TEM) and Fourier-transform infrared (FTIR) spectroscopy. By increasing the amount of ZnO-N filler in PNCs, a huge difference in properties was observed especially on relative dielectric constant and electrical conductivity. As the ZnO-N filler content was increased to 10% of total solid, the electrical conductivity and relative dielectric constant of PNCs were observed to increase by 53% (to  $0.95 \mu\text{S cm}^{-1}$ ) and 60% (to 44.1), respectively. The tangent loss in PNCs without filler was measured to be 78% larger (at 7.3) than that of BNC film (at 1.6) with 10% filler content. The highest obtainable room temperature conductivity was  $0.95 \times 10^{-6} \text{ S cm}^{-1}$  for sample with 10 wt% ZnO-N filler. FESEM micrographs showed no particles agglomeration of ZnO-N in all film samples indicating a uniform distribution of nanoparticles inside the polymer films. Ultraviolet (UV) absorbance shows total absorption of light below 380 nm in all film samples except control film. PNCs with ZnO-N also show zero light transmission below 380nm. FTIR analysis revealed that there was no presence of new functional groups after the application of ZnO-N into PNCs samples indicating that the interaction between ZnO-N and SS polymer was physical in nature.*

**Keywords:** Polymer nanocomposites, zinc oxide nanorods, relative dielectric, tangent loss, UV absorbance, UV transmission

### 1. INTRODUCTION

Interest in the study of biopolymer system has been continuously growing in recent years due to the various potential applications such as in

electronics,<sup>3</sup> medical,<sup>4</sup> food packaging,<sup>5</sup> bioplastics<sup>6</sup> and coating.<sup>7</sup> Characteristics such as being biosafe, renewable, biodegradable and carbon neutral have made application of biopolymer important in production of environmental friendly product.<sup>1,2</sup> However, conventional polymer has been reported to have a few limitations in their properties. Research suggested that addition of inorganic nanofiller into the polymer will result in enhancement of polymer properties, which greatly differ from the conventional polymer and exhibit unexpected properties.<sup>8-11</sup> Therefore, different types of nanofiller have been produced for this purpose. Some of the most reported metal oxide inorganic nanofillers in the literature include TiO<sub>2</sub>, Al<sub>2</sub>O<sub>3</sub>, SiO<sub>2</sub> and ZnO.<sup>12-15</sup>

ZnO-N is a multifunctional n-type semiconductor that has a wide band gap (3.4 eV), large exciton binding energy (60 meV), effective ultraviolet absorbance and good chemical stability.<sup>18</sup> It shows great potential in application of solar cell,<sup>12</sup> gas sensor,<sup>19,20</sup> varistor,<sup>21</sup> cosmetic material<sup>22</sup> and so on. ZnO is reported to be nontoxic and environmental friendly which makes it valuable for bio-application.<sup>23</sup> In addition, ZnO also exhibits anti-bacterial properties that are useful for pharmaceutical application. Starch, on the other hand, is an organic compound which can be found commonly in food. It was known for its use in textile and food industries for decades. Biocompatibility properties of starch have driven more research group to work on this material for various types of applications including in medical<sup>16</sup> and pharmaceutical.<sup>17</sup> A recent application of starch is in pharmaceutical capsules as a potential replacement for the conventional animal gelatin capsule. However, application of starch-based polymer in food packaging may not be suitable due to its limitation especially the anti-bacterial properties of the polymer. Therefore, the main purpose of having ZnO-N incorporated in starch-based polymer is to improve the quality of the end product in terms of anti-bacterial properties.

As reported in literature, ZnO nanoparticles carry proven anti-bacterial properties. Many research groups reported to have ZnO nanoparticles in the inhibition of bacteria growth.<sup>29</sup> However, the exact in-action mechanism of ZnO nanoparticles is still unknown. Zhang et al. suggested that bacteria inhibition occurs through direct interaction between ZnO nanoparticles and the cell surface.<sup>31</sup> This interaction affects the cell membrane permeability, causing the nanoparticles to enter the cell system and inducing the oxidative stress in the bacterial cell. This will result in the inhibition of bacterial growth and cause bacterial death. Since the ZnO nanoparticles are trapped between the polymer matrix after incorporation with PNCs, the suggestion does not seem suitable to describe the anti-bacterial mechanism of ZnO nanoparticles in starch-based PNCs. This is because the trapped ZnO nanoparticles are not capable to enter the cell system and inhibit the bacterial growth.

Zhang et al. also suggested another cause of bacteria inhibition, which is the electrostatic force interaction between ZnO nanoparticles and cell surface.<sup>31</sup> This interaction will create opposing charges between the bacteria and nanoparticles that will generate an electrostatic force. This electrostatic force will strongly bind the bacteria and ZnO nanoparticles together and consequently cause cell membrane damage. This suitably describes the anti-bacterial properties of ZnO nanoparticles in PNCs, since ZnO nanoparticles are an n-type semiconducting material which unintentionally carries charge carrier in each individual particle. On the other hand, the behaviour of charge carrier in SS/ZnO-N PNCs has not been reported before. Further, their behaviour under the influence of frequency with different concentration of ZnO nanoparticles is still unknown. For this purpose, analysis on relative dielectric, electrical conductivity and tangent loss properties of SS/ZnO-N PNCs have been performed. The aim of these studies is to get a better understanding on the electrical behaviour of charge carrier in PNCs with different concentration of ZnO-N, which then will contribute to the anti-bacterial properties of SS/ZnO-N PNCs. The relations between these properties have been clearly described in the results and discussion part.

Besides electrical, ZnO nanoparticles also exhibit promising optical behaviour that may contribute to the anti-bacterial properties of SS/ZnO-N PNCs. Many research groups reported having ZnO nanoparticles in UV-shielding applications. Since conventional polymer such as starch cannot provide UV-shielding capability, the incorporation of ZnO nanoparticles in starch-based PNCs are expected to provide this property. Therefore, studies on starch-based polymer nanocomposites on UV shielding with presence on ZnO-N at different filler concentration has been done in order to get better understanding on how different concentrations of ZnO-N will effect the UV absorption and transmission of PNCs.

## 2. EXPERIMENTAL

Nano zinc oxide was synthesised using a method introduced by Shahrom et al. known as catalyst-free combust-oxide mesh (CFCOM) process.<sup>32</sup> Sago starch (13.4% moisture), food grade glycerol and liquid sorbitol were obtained from SIM Company Sdn. Bhd. (Penang, Malaysia). ZnO-N powder was dispersed in water at different concentrations (2, 4, 6, 8 and 10%, w/w of total solid) and mixed with 40% (w/w of total solid) of sorbitol and glycerol (3:1). Film without addition of ZnO-N served as control. The choice and ratio of plasticiser used was based from Abdorreza et al. and the concentration of plasticiser applied was constant throughout all samples.<sup>33</sup> The mixture was sonicated in ultrasonic bath (Marconi model, Unique USC 45 kHz, Piracicaba,

Brazil) for 10 min. Then, 4% (w/w) of sago starch were mixed with the ZnO-N solution and heated up to  $90 \pm 5^\circ\text{C}$  for 45 min with constant agitation. Upon completion, the solution was cooled down to room temperature and the solution was cast on Perspex plate fitted with rims around the edge. The thickness of samples was controlled through weight-control method, where  $90 \pm 2$  g of solution was cast on Perspex plate. The average thickness of each sample was  $0.14 \pm 1$  mm. The yield area of film formation was  $16 \times 16$  cm<sup>2</sup>. The cast solution were placed in an oven at  $40^\circ\text{C}$  for 24 h and then were peeled and stored at room temperature with  $50 \pm 5\%$  relative humidity (RH). The thickness of BNCs film was measured before tested at five different location centre and edge to the nearest 0.01 mm using digital micrometer screw gauge (Mitutoyo, Tokyo, Japan).

The structure of zinc oxide nanorods were examined using TEM before embodiment with starch-based polymer. Dispersion of ZnO-N after embodiment with starch-based polymer was examined using Gemini Supra 50 VP FESEM. Energy dispersive X-ray spectroscopy (EDX) was used to detect type of element present in PNCs and analysis of ZnO-N interaction with starch-based polymer has been performed using FTIR spectrometer model Perkin Elmer Spectrum GX in spectra range between 400 and 4000 cm<sup>-1</sup>. UV absorption and transmission have been performed using Shimadzu UV-1800 UV-Vis spectrometer in the range of wavelength 1100 to 250 nm. The dielectric permittivity, conductivity and tangent loss properties of starch-based polymer nanocomposites were examined using Agilent 4284a Precision LCR meter in frequency range between 0.01 kHz and 1000 kHz.

### **3. RESULTS AND DISCUSSION**

#### **3.1 FESEM and TEM Analysis**

The TEM micrographs of zinc oxide nanorods are as shown in Figure 1(a) and (b). The TEM micrographs shows ZnO-N having widths of 30–100 nm and lengths of 100–300 nm. The physical looks of SS/ZnO-N PNCs with different filler concentration were shown in Figure 1(c). It can be observed that as concentrations of nanoparticles reduce, the PNCs tend to become transparent. As suggested by literature, light penetration capability through polymer composites is dependent on inter-particle distance and structure of the filler.<sup>30</sup> High concentration of filler is reported to result in formation of filler multilayer inside the polymer that reduces the intensity of light passing through polymer films. Besides multilayer effect, it was also suggested that the inter-particle distance of nanofiller decreases as the amount of nanofiller in polymer nanocomposites increases. Figure 1(d) shows the elemental peak of PNCs composition using EDX. Figure 1(e) shows a dispersion of ZnO-N at the cross section of PNCs film

with 10% (w/w of total solid) filler content. It can be seen that no agglomeration of nanoparticles were observed in PNCs film. The EDX analysis as in Figure 1(d) shows zinc (Zn), oxygen (O) and carbon (C) were presence in PNCs and no impurities were detected. The results also suggest that carbon having the highest percentage in PNC composition. It is due to the nature of organic composition, which is made up of carbon. Presence of gold (Au) was due to the coating of samples for SEM purpose.

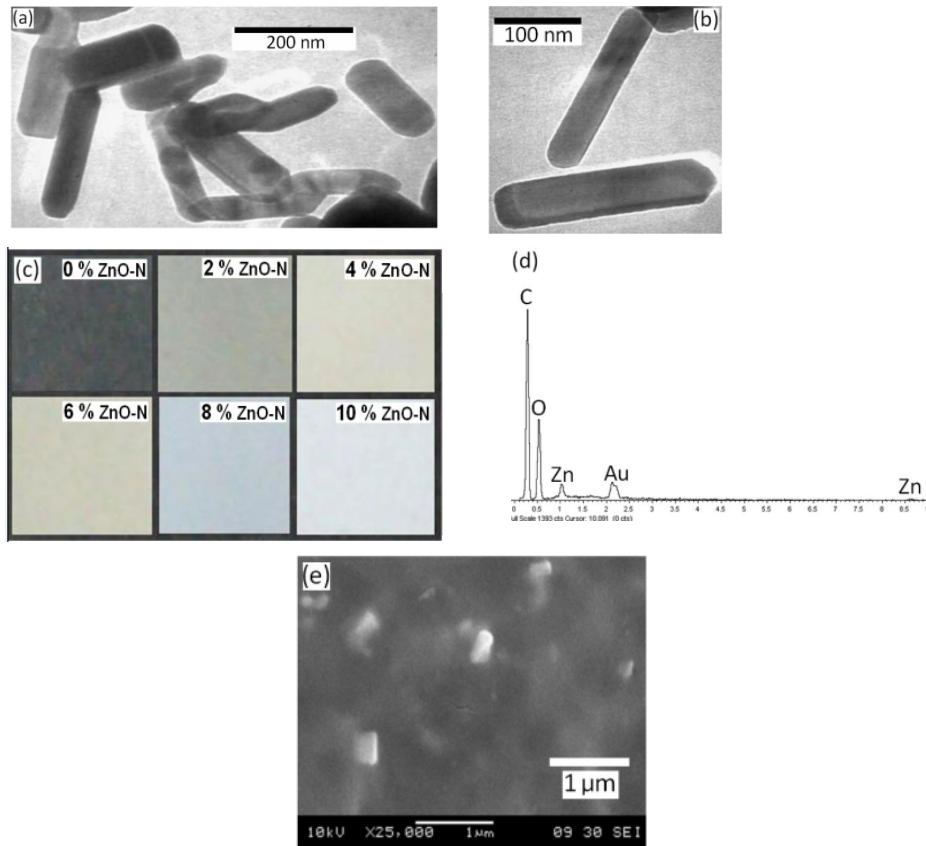


Figure 1: Illustration of (a) and (b): TEM micrographs of ZnO nanorods; (c) SS/ZnO-N BNCs with different filler content; (d) EDX elemental analysis; and (e) nanoparticles dispersion of ZnO-N in BNCs with 10% filler concentration.

### 3.2 FTIR and UV-Vis Analysis

The study shows that SS/ZnO-N bionanocomposite with different filler concentration demonstrate the same spectra in the range of wavenumber 400 to 4000  $\text{cm}^{-1}$ . As the concentration of ZnO-N increases in BNCs, neither sharpening nor shifting was detected. It reveals that only physical interaction between ZnO-N filler and starch-based polymer was taking place in polymer nanocomposites. The FTIR spectra of the polymer nanocomposites with different ZnO-N filler concentration are shown in Figure 2(a). Figure 2(b) and (c) show the absorption and transmission spectra of SS/ZnO-N PNCs in the range of wavelength 1100 to 250 nm. The absorption spectra in Figure 3(b) show that the amount of light absorbed by PNCs increased as the wavelength was reduced. In addition, more light was absorbed as the concentration of filler in PNCs increased. The absorbance level was observed to peak between the wavelength range of 360 and 375 nm. These results indicate that the SS/ZnO-N PNCs exhibit an obvious blue-shift phenomenon. Similarly, the amount of light transmitting through the PNCs was reduced as the amount of filler concentration increased. Therefore, it is suggested that the presence of ZnO-N in starch-based polymer improved the UV-shielding property of the polymer. This property is important especially in the application of pharmaceutical capsules since the drug inside the capsules can be protected from unwanted rays that might change its properties or cause damage.

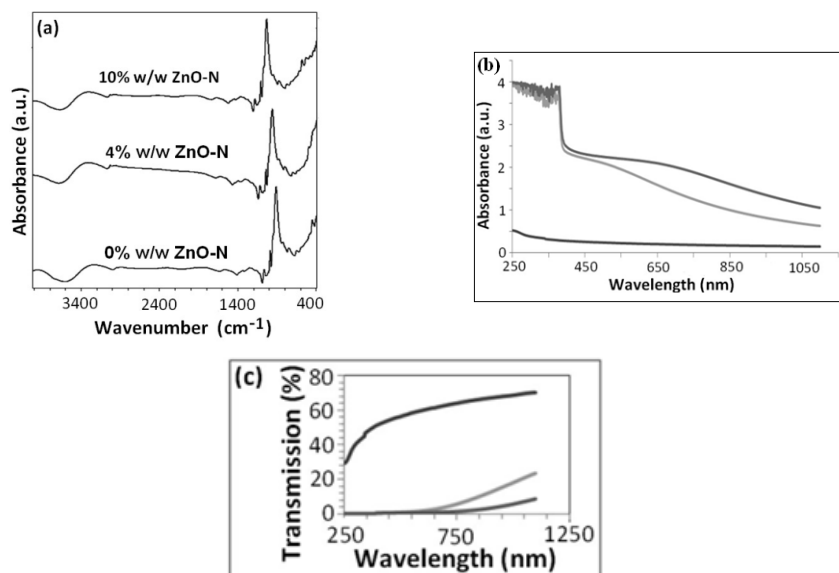


Figure 2: Illustration of (a) FTIR spectra; (b) UV-Vis absorption; and (c) UV-Vis transmission of SS/ZnO-N BNCs at different filler concentration.

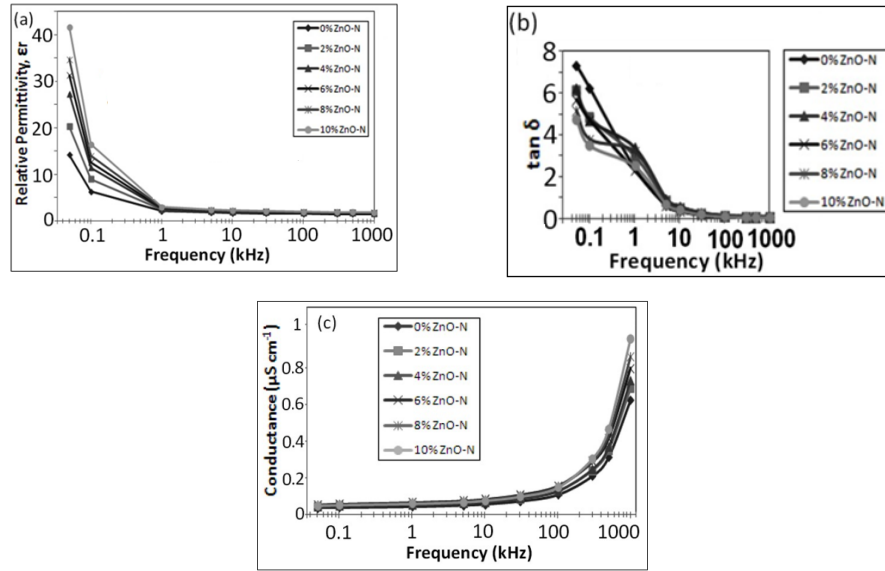


Figure 3: Illustration of (a) relative permittivity behaviour; (b) dielectric loss; and (c) conductance in a function of frequency of SS/ZnO-N BNCs.

### 3.3 Dielectric and Tangent Loss Behaviour

The term relative permittivity ( $\epsilon_r$ ) or dielectric constant ( $k$ ) was known to describe the dielectric permittivity of free space. The dielectric response of the nanofiller in the bionanocomposite at various frequencies is described in term of complex permittivity ( $\epsilon^*$ ) which is represented by a real and imaginary part.

$$\epsilon^* = \epsilon' - i\epsilon'' \quad (1)$$

where  $\epsilon'$  is the dielectric permittivity and  $\epsilon''$  is the dielectric loss. The dielectric loss tangent ( $\tan \delta$ ) is defined as

$$\tan \delta = \frac{\epsilon''}{\epsilon'} \quad (2)$$

The relative permittivity as a function of frequency for different ZnO-N concentrations at room temperature is compared in Figure 3(a). Dispersion of permittivity over frequency was observed in low frequency region followed by a nearly frequency independent behaviour above 1 kHz. There is a significant effect of ZnO-N on  $\epsilon_r$  value of PNCs at lower frequency region. The permittivity of the unfilled polymer obtained is less than the polymer with filler where it

shows a significant change as the concentration of filler increased. The values of permittivity reduce over a wide range of frequencies but further increase in filler loading will result in an increase in permittivity values. The embodiment of ZnO-N filler in polymer nanocomposites may result in more localisation of charge carriers along with mobile ion and this produces higher  $\epsilon_r$  value with strong low frequency dispersion.<sup>25,26</sup> Literature has reported that interactions between nanofiller with polymer chain may also affect the values of effective permittivity. The physical interaction may result in hindrances of the mobility of nanocomposite and this may contribute to lower value of relative permittivity and conductivity.<sup>27</sup> However, the physical interaction between ZnO-N filler and SS polymer shows encouraging behaviour of relative permittivity where higher  $\epsilon_r$  value was obtained as concentration of filler increased. Hence, it suggests that the interaction between ZnO-N filler with SS polymer does not preclude in mobility of PNCs. The decrease in relative permittivity,  $\epsilon_r$  with frequency may attribute to the electrical relaxation process.

Figure 3(b) shows the variation of loss tangent with frequency at different concentrations of ZnO-N in PNCs at room temperature. At low frequency region below 1 kHz, it can be observed that the loss tangent of unfilled polymer is higher compared to biopolymer with filler. In general,  $\tan \delta$  values are expected increase as concentration of filler in the material increase. However, such observation could not be made here. Literature reported that such cases can occur due to the charge transport through different chain or interfaces and defects.<sup>26,27</sup> At lower nanofiller loading, the number of nanofiller present in polymer is less. Hence, less free charge carriers from filler are present in PNCs. In this case, the inter-particle distances are high and this may result in higher charge trapping sites, which reduce the conducting path. These conditions increase the probabilities of charge trapping and charge neutralisation. It reflects the condition where at lower nanofiller loading, the tangent delta obtained is similar or less than the unfilled polymer. Whereas, higher nanofiller loading will result in higher free charge carriers from the nanofiller to accumulate in the polymer. This condition may reduce the inter-particle distance of nanofiller and decrease the charge trapping sites and probability of charge neutralisation. Hence, higher electrical conduction behaviour of PNCs will be obtained and these conditions result in the tangent loss to be significantly smaller than that of unfilled polymer.

### 3.4 Conductivity of SS/ZnO-N Bionanocomposite

Figure 3(c) shows the variation of conductivity,  $\sigma$  with variation of frequency at different concentration of ZnO-N filler. The conductivity of unfilled polymer obtained is less than that of polymer with filler where significant changes were observed as the concentration of filler increases. The conductivity



exhibits a nearly frequency-independent behaviour at low frequency region and dispersion at higher frequency. Further increase in filler loading will increase the conductivity values, which keep increasing over a wide range of frequencies. The maximum conductivity of  $0.95 \times 10^{-6} \text{ S cm}^{-1}$  was achieved for samples with 10% (w/w, of total solid) filler content. There are various factors that may influence the conductivity which include the number of charge carriers, mobility of free charge and the availability of connecting the polar domain as the conduction pathway.<sup>28</sup>

In the case of bionanocomposite, the increase in conductivity values could be attributed to the increment of charge carrier due to the embodiment of ZnO-N filler in bionanocomposite. The variation of SS/ZnO-N bionanocomposites conductivity was observed to follow the universal dynamic response as suggested by the literature. The nature of universal dynamic response has been widely observed in disordered materials like conducting polymers and conducting glass. According to jump relaxation model at very low frequency ( $\omega \rightarrow 0$ ) an ion can jumps from one sites to its neighbouring vacant site. Such behaviour may contribute to the occurrence of DC conductivity. However, at higher level of frequencies the probability for the ion to go back again to its initial sites increases due to the short time periods available. Table 1 shows the overall electrical behaviour of SS/ZnO-N polymer nanocomposites.

Table 1: Dielectric and conductance behaviour of SS/ZnO-N bionanocomposites.

ZnO-N (%)	Relative permittivity, $\epsilon$	Tangent loss, $\delta$	Conductance ( $\mu\text{S cm}^{-1}$ )
	[At $f = 0.01 \text{ kHz}$ ]	[At $f = 0.01 \text{ kHz}$ ]	[At $f = 1 \text{ MHz}$ ]
0	14.4	7.3	0.61
2	20.5	6.2	0.69
4	28.5	6.1	0.73
6	33.8	5.9	0.80
8	39.0	5.2	0.82
10	44.1	4.9	0.95

#### 4. CONCLUSION

Incorporation of ZnO-N as nanofiller in the polymer nanocomposites plays an important role in enhancing their electrical and optical properties. Adding low-level nanofiller concentration in PNCs will result in a huge difference in both properties. The optical properties showed an improvement especially on absorption and transmission of light in blue region. This suggests that the presence of ZnO-N in starch-based polymer can provide UV-shielding

properties to conventional starch polymers. Besides optical properties, SS/ZnO-N PNCs also showed promising electrical properties. From the results, the charge carriers of ZnO-N in starch-based polymer are present along with the addition of ZnO-N. Their behaviour varied with the concentration of ZnO-N and frequency applied. The localisation of charge carriers in the polymer suggests that the mechanism of anti-bacterial of SS/ZnO-N PNCs can be achieved. This is due to enhancement of the anti-bacterial properties of starch-based polymer through electrostatic discharge between ZnO-N and bacteria. However, in order to prove that the localisation of charge carriers in starch-based polymer may preclude the growth of bacteria, further research such as *in-vitro* studies is required. As a conclusion, the early studies on optical and electrical properties of ZnO-N presence in conventional polymer such as starch-based polymer is proven to improve the UV shielding and provide localisation of charge carriers, hence improving the electrical properties of conventional polymer.

## 5. ACKNOWLEDGEMENT

The authors acknowledge the Universiti Sains Malaysia (USM) for a research grant (1001/PFIZIK/814174) and School of Physics, School of Industrial Technology, and School of Material and Mineral Resources Engineering for providing research facilities.

## 6. REFERENCES

1. Zareh, E. N., Moghadam, P. N., Azariyan, E. & Sharifian, I. (2011). Conductive and biodegradable polyaniline/starch blends and their composites with polystyrene. *Iran. Polym. J.*, 20(4), 313–328.
2. Lu, D. R., Xiao, C. M. & Xu, S. J. (2009). Starch-based completely biodegradable polymer materials. *eXPRESS Polym. Lett.*, 3(6), 366–375.
3. Singh, B., Sariciftci, S., Grote, J. & Hopkins, F. (2006). Bio-organic-semiconductor field-effect transistor (BiOFET) based on deoxyribonucleic acid (DNA) gate dielectric. *J. Appl. Phys.*, 100(2), 1–4.
4. Stodolak, E., Paluszkiwicz, C., Bogun, M. & Blazewicz, M. (2009). Nanocomposite fibers for medical applications. *J. Mol. Struct.*, 924–926, 208–213.
5. Maizurah, M., Fazilah, A., Norziah, M. H. & Karim, A. A. (2007). Antibacterial activity and mechanical properties of partially hydrolyzed sago starch-alginate edible film containing lemongrass oil. *J. Food Sci.*, 1(2), 1–7.
6. Domenek, S. et al. (2004). Biodegradability of wheat gluten based bioplastics. *Chem.*, 54(1), 551–559.

7. Vila, M. et al. (2011). Novel biopolymer-coated hydroxyapatite foams for removing heavy-metals from polluted water. *J. Hazard Mater.*, 192(1), 71–77.
8. Gacitua, W., Ballerini, A. & Zhang, J. (2005). Polymer nanocomposites: Synthetic and natural fillers a review. *Cien. Technol.*, 7(3), 159–178.
9. Singha, S. & Thomas, M. J. (2009). Influence of filler loading on dielectric properties of epoxy-ZnO nanocomposites. *IEEE Trans. Dielectr. Electr. Ins.*, 16(2), 1070–9878.
10. Fazilah, A. et al. (2011). Physical and mechanical properties of sago starch incorporated with calcium chloride. *Int. Food Res. J.*, 18(3), 1027–1033.
11. Khiar, A. S. A. & Arof, A. K. (2011). Electrical properties of starch/chitosan-Nh<sub>4</sub>no<sub>3</sub> polymer electrolyte. *World Aca. Sci. Eng. Tech.*, 59(1), 23–27.
12. Wang, Z. S. et al. (2001). A highly efficient solar cell made from a dye-modified ZnO-covered TiO<sub>2</sub> nanoporous electrode. *Chem. Mater.*, 13(1), 678–682.
13. Hirvikorpi, T. et al. (2011). Thin Al<sub>2</sub>O<sub>3</sub> barrier coating onto temperature-sensitive packaging material by atomic layer deposition. *Surf. Coat. Tech.*, 205(1), 5088–5092.
14. Chu, H. Q., Yu, C., Wan, Y. & Zhao, D. (2009). Synthesis of ordered mesoporous bifunctional TiO<sub>2</sub>-SiO<sub>2</sub>-polymer nanocomposites. *J. Mater. Chem.*, 19, 8610–8618.
15. Lupan, O. et al. (2008). Biopolymer-assisted self-assembly of ZnO nanoarchitectures from nanorods. *Superlatt. Microstruct.*, 43(2), 292–302.
16. Latner, A. L. & Zaki, A. H. (1960). Clinical uses of starch gel electrophoresis with special reference to leukaemia. *Clin. Chim. Acta*, 5(1), 22–25.
17. Won, C-Y., Chu, C-C. & Yu, T-J. (1997). Synthesis of starch-based drug carrier for the control/release of estrone hormone. *Carbohydr. Polym.*, 32, 239–244.
18. Janotti, A. & Van de Walle, C. G. (2009). Fundamentals of zinc oxide as a semiconductor. *IOP Publ.*, 72, 126501, doi:10.1088/0034-4885/72/12/126501.
19. Yi, G. C., Wang, C. & Park, W. I. (2005). ZnO nanorods: Synthesis, characterization and applications. *Semicon. Sci. Technol.*, 20(2), 22–34.
20. Baruwati, B., Kumar, D. K. & Manorama, S. V. (2006). Hydrothermal synthesis of highly crystalline ZnO nanoparticles: A competitive sensor for LPG and EtOH. *Sens. Actua. B*, 119, 676–682.
21. Li, Y., Li, G. & Yin, Q. (2006). Preparation of ZnO varistors by solution nano-coating technique. *Mater. Sci. Eng.*, 130, 264–268.

22. Iwasaki, T., Satoh, M., Masuda, T. & Fujita, T. (2000). Powder design for UV-attenuating agent with high transparency for visible light, *J. Mater. Sci.*, 35(1), 4025–4029.
23. Zhou, J., Xu, N. S. & Wang, Z. L. (2006). Dissolving behavior and stability of ZnO wires in biofluids: A study on biodegradability and biocompatibility of ZnO nanostructures. *Adv. Mater.*, 18(2), 2432–2435.
24. Hong, J. I., Winberg, P., Schadler, L. S. & Siegel, R. W. (2005). Dielectric properties of zinc oxide/low density polyethylene nanocomposite. *Mater. Lett.*, 59, 437–476.
25. Baskaran, R., Selvasekarapandian, S., Hirankur, G. & Bhuvaneswari, M. S. (2004). Vibrational, AC impedance and dielectric spectroscopic studies of poly(vinylacetate)-*N,N*-dimethylformamide-LiClO<sub>4</sub> polymer gel electrolytes. *J. Power Source*, 134(2), 235–240.
26. Nelson, J. K. & Fothergill, J. C. (2004). Internal charge behavior of nanocomposites. *Nanotech.*, 15(1), 586–595.
27. Levinson, L. M. & Philipp, H. R. (1976). AC Properties of metal oxide varistors. *J. Appl. Phys.*, 47(3), 1117–1122.
28. Funke, K. & Hoppe, R. (1990). Jump-relaxation model yields Kohlrausch-Williams-Watts behaviour. *Sol. State Ion.*, 40(1), 200–204.
29. Espitia, P. J. P. et al. (2012). Zinc oxide nanoparticles: Synthesis, antimicrobial activity and food packaging applications. *Food Bioproc. Technol.*, 5(1), 1447–1464.
30. Gluba, T. & Kochanski, B. (2000). Interparticle distance in the cross section of granules with different grain size distributions. *Physicochem. Prob. Min. Process.*, 34(1), 57–66.
31. Zhang, L. L. et al. (2007). Investigation into the antibacterial behavior of suspensions of ZnO nanoparticles (ZnO nanofluids). *J. Nanopart. Res.*, 9, 479–489.
32. Mahmud, S. et al. (2006). Growth model for nanomallets of zinc oxide from a catalyst-free combustoxidised process, *J. Cryst. Growth*, 287(1), 118–123.
33. Mohammadi Nafchi, A., Alias, A. K., Mahmud, S. & Robal, M. (2012). Antimicrobial, rheological, and physicochemical properties of sago starch films filled with nanorod-rich zinc oxide. *J. Food Eng.*, 113(4), 511–519.